Change in site-specific shape resonance of nitrogen K-shell photoionization induced in hot-N_2O molecules

M Hoshino[1], H Kato[1], N Kuze[1], H Tanaka[1], H Fukuzawa[2], K Ueda[2] and R R Lucchese[3]

[1] Department of Materials and Life Sciences, Sophia University, Tokyo 102-8554, Japan
[2]Institute of Multidisciplinary Research for Advanced Materials, Tohoku University, Sendai 980-8577, Japan
[3] Department of Chemistry, Texas A&M University, College Station, TX 77843-3255, USA

E-mail: masami-h@sophia.ac.jp (M. Hoshino)

Abstract. The central (N_c) and terminal (N_t) nitrogen K-shell photoelectron spectra (PESs) of N_2O molecules have been measured in the σ shape resonance energy region at temperatures of ~300 K and ~630 K. Estimating vibrational populations based on the Boltzmann distribution at these temperatures, PESs of vibrationally-ground and bending-excited levels in the initial electronic ground state were extracted. Vibrationally-integrated partial cross sections and asymmetry parameters from vibirationally-ground and bending-excited levels were obtained as a function of incident photon energy by integrating PESs over the vibrational levels of the core-hole states. For the N_c photoionization, the shape resonance from the bending-excited level was found to be shifted to the lower photon energy side and to become narrower than that from the vibrationally-ground level, whereas for the N_t photoionization from the bending-excited level, downward shift of the resonance is more significant than that of the N_c ionization. These experimental findings are qualitatively consistent with the theoretical predictions and suggests that the shape resonance associated with the N_t core hole is more sensitive to the bending angle of the initial state than that of the N_c core hole. The asymmetry parameters from the bending-excited level, however, showed almost the same behavior as those from vibrationally-ground level for both K-shell photoionization in the studied photon energy range.

Keywords: X-ray photoelectron spectroscopy, inner-shell ionization cross sections, asymmetry parameters, vibrationally-excited N_2O molecule, and hot-molecules.

(Some figures may appear in colour only in the online journal)

1 Introduction

Shape resonances are common phenomena in low-energy electron scattering and photoionization of molecular targets in the energy region below ~ 50 eV [1]. The shape resonance is caused by the dynamical trapping of an incident electron or a photoelectron in the effective potential of molecular targets, which was formed by the combination between a generally attractive electron-molecule (or ion) interaction potential and a repulsive potential from a centrifugal force. Dehmer et al. predicted that the energy of the shape resonance observed in photoionization depends on which vibrational level is produced in the molecular ion because the shape resonance energy is intrinsically sensitive to the internuclear distances in a molecule [2]. High-resolution measurements for core-level photoelectron spectra (PES) of molecules carried out on soft x-ray beamlines at the third generation synchrotron radiation light sources revealed the distribution of the vibrational levels in the core-hole state and the photoelectron angular distribution vary in the shape resonance region. Such studies have been predicted by Dehmer et al. [2] and reported for CO [3], H_2CO [4], N_2 [5], C_2H_2 [6], CO_2 [7,8] and NO [9].

Nitrous oxide (N_2O) plays an important role in different enviroments where its main relevance has been recognized on atmospheric chemistry studies [10]. N_2O can be released in the atmosphere from planets proving a relevant a principal control mechanism limiting the O_3 concentration in the ozone layer [10]. N_2O is a prototypical example molecule for studying shape resonances in the inner-shell photoionization region because it bridges a gap between simple diatomic molecules and complex polyatomic molecules [11]. N_2O has two nitrogen atoms in different sites, labelled as central nitrogen (N_c) and terminal nitrogen (N_t) (N_t-N_c-O). The K-shell binding energies of N_c and N_t are different due to the differences in chemical shifts for those two atoms. Previously, we reported both experimental and theoretical vibrationally-resolved partial cross sections and asymmetry parameters for the N_c and N_t K-shell photoionization of the N_2O molecule in the σ shape resonance region [12]. We found that the excitation photon energies of the shape resonances associated with the N_c and N_t core holes are almost the same (~426 eV) instead of being different by ~4 eV which is the difference in chemical shifts of corresponding core hole states. We also successfully extracted the variation of the shape resonance with final vibrational quantum number in the vibrationally-resolved photoionization cross sections of the N_c and N_t core-hole states, which is a measure of the dependence photoionization cross section on the internuclear distance in the final ionic states.

Hot-molecules, i.e., molecules partly vibrationally-excited, have received much attention in the past. They opened new avenues to study properties of target molecules that emerge by the vibrational excitation since it may break the symmetry and/or enhance vibronic coupling effects. Some of the present authors reported measurements of low-energy electron energy loss spectroscopy (EELS) on hot-CO_2 [13], hot-N_2O [14] and hot-COS [15] molecules. In these investigations, the absolute differential cross sections of the inelastic and super-elastic vibrational excitations were measured as a function of incident electron energy and the influence of vibrational excitation of the target molecule on the shape resonance such as $^2\Pi_g$ at ~3.8 eV for CO_2, $^2\Pi$ at ~2.3 eV for N_2O, and Π at ~1.3 eV for COS were discussed. The experimental data available in the literature for the vibrationally-excited hot

molecules are, however, still limited due to the difficulty in producing a sufficient number of excited species.

The above described work on hot molecules was inspired by the results of symmetry-resolved x-ray absorption spectroscopy on hot-CO_2 [16], hot-N_2O [17] and hot-CF_3I [18] recorded at SPring-8, an 8-GeV synchrotron radiation facility in Japan. In Refs. 16 and 17, the angle-resolved ion yield (ARIY) spectra in $C1s^{-1}2\pi_u$, $O1s^{-1}2\pi_u$, and $N1s^{-1}3\pi$ resonances for CO_2 and N_2O, respectively, were recorded at room (300 K) and at a high (~630 K) temperatures. From these spectra, symmetry-resolved absorption profiles for the vibrationally-ground and bending-excited levels were extracted. The absorption spectra for the bending-excited level exhibited dramatic changes from those of the vibrationally-ground level, reflecting that a different part of the potential energy surface of the core-excited state was probed.

We also measured also the initial vibrational-level-specific ARIY spectra of CO_2 and N_2O in the shape resonance regions above the K-shell ionization threshold using the same experimental technique, which were compared with calculations employing the Schwinger variational principle [19]. These results showed that significant diminution of the shape resonances by the bending excitation in the initial electronic ground state was observed. However, in that study we could not resolve the shape resonances associated with N_c and N_t core holes.

In the present work, we have extended the previous core-level photoemission study on N_2O at room temperature [12] and ARIY measurements of hot-N_2O [18] to core-level photoemission study on hot-N_2O. Here we aim at investigating the influence of the bending excitation in the initial ground electronic state on the shape resonances associated with N_c and N_t core holes that were not resolved in the previous ARIY measurements. In addition, we aimed at extracting the variation of the shape resonance in the photoionization region from the bending excited N_2O as a function of vibrations in N_c and N_t core holes. Accidental overlap of different vibrational progressions and also low statistics of the present PES data stemming from the low density of the vibrational excited molecules, however, did not allow us to extract such detailed information. We also calculated the initial-vibrational-specific-cross sections and asymmetry parameters for N_c and N_t K-shell ionizations in N_2O based on the equivalent-core Hartree Fock (ECHF) method.

In the next section, we describe our experimental and analysis procedures. In Sec. 3, we present a brief description of the additional computation in this work and provide a discussion in addition to the present set of experimental results. Finally, conclusions from this work are presented in Sec. 5.

2 Experimental details

2.1 General

The experiments were carried out on the C-branch of the soft x-ray photochemistry beam line 27SU at SPring-8 in Japan. Details of this beam line were reported elsewhere [20-22]. Briefly, the radiation source is a figure-8 undulator providing radiation linearly polarized either in the horizontal plane of the storage ring (1^{st} order) or in the vertical plane that is perpendicular to the plane of the storage ring (0.5^{th} order) [23]. Thus angle-resolved photoelectron emission measurements at 0^o and 90^o

with respect to the linear polarization axis are performed only by changing the undulator gap without rotating the electron analyzer. The electron spectrometer consists of a hemispherical electrostatic analyzer (Gammadata-Scienta SES2002), a differentially pumped chamber, and a newly added gas heating source.

The degree of linear polarization was already determined by observing Ne 2s and 2p photolines and confirmed to be greater than 0.98 with the present setting of optics [24]. In the present analysis, we assumed complete polarization of the incident light at the photon energies employed. The photon flux was measured by the photocurrent detector on the refocusing mirror and a gold foil installed before and after the gas source. The target pressure was monitored by a pressure gauge in the vacuum chamber. The photon energy scale was calibrated relative to the maximum of the $N1s^{-1}3\pi$ resonant peak of the N_2O molecule [25].

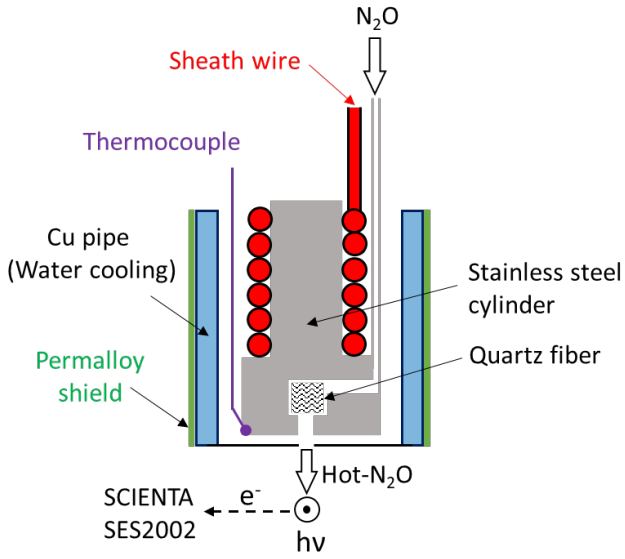

Figure 1. Schematic view of our hot-N_2O source.

Vibrationally-excited N_2O molecules were produced by a resistive heating technique. The gas heating system was newly developed at Sophia University. The basic principle is similar to the heating system used in the electron scattering measurements [15]. N_2O gas is heated by using a cylindrical K-cell (a Kunudsen cell) made of solid stainless steel with a 5 mm long nozzle and 0.8 mm diameter drilled through the conical top. The K-cell is filled with fluffy quartz fibers to attain better thermal equilibrium which is heated by wrapping it with a resistive coaxial sheath wire, and can reach temperatures up to about 800 K. A calibrated thermocouple was set near the head of nozzle to monitor the cell temperature. This cell is surrounded by a water-flowing copper pipe to minimize heat penetration into the interaction region and the spectrometer. Magnetic fields in the region of the K-cell are reduced to less than a few mG by covering with a permalloy shield. Note that in the present data analysis, we assumed the molecular gas temperature was the same as the temperature measured by the thermocouple (~300 K and ~630 K) because an effusive molecular beam (not a supersonic source) is

produced from the K-cell in a thermal equilibrium state and intersects a photon beam at right angular (about 2.5 mm below the nozzle, see figure 1). This assumption was validated by observing the super-elastic peak (deexcitation from the N_2O bending-excited mode) clearly in the electron energy loss spectroscopy. The variation of target density with increasing temperature in the interaction region with the photon beam was corrected by measuring the Ar 2p photoelectron spectra as a function of the monitored temperatures, since the cross sections of photoionization for the atomic target are independent of the temperature. This is the same method as used in the previous electron energy loss spectroscopic study of hot-N_2O [14]. The correction factor between the room temperature and ~630 K was estimated experimentally to be about 1.3 in the present measurement.

Figure 2 depicts N_c and N_t core-level photoelectron spectra (PESs) for N_2O at a photon energy of 421.1 eV, i.e., 8.64 eV above the N_c *K*-shell ionization threshold and 12.66 eV above the N_t threshold [26]. The PESs I_{room}(300K) and I_{hot}(630 K) were recorded at room temperature (~300 K) and at a high temperature (~630 K), respectively. Note that the PESs in figure 2 were obtained from spectra recorded at 0^o and 90^o converting them to the PESs at the magic angle of 54.7^o according to the equation, $I(54.7^o) = I(0^o) + 2\times I(90^o)$, which assumes 100% linear polarization. Here the relative intensities of $I(0^o)$ and $I(90^o)$ were corrected for the monitored photon flux and target gas pressure. Furthermore, the relative intensities of I_{room}(300K) and I_{hot} (630 K) in figure 2 were corrected by the factor of 1.3 as described above. We have recorded such PESs at two different temperatures at six different photon energies in the range of 419 eV – 430 eV.

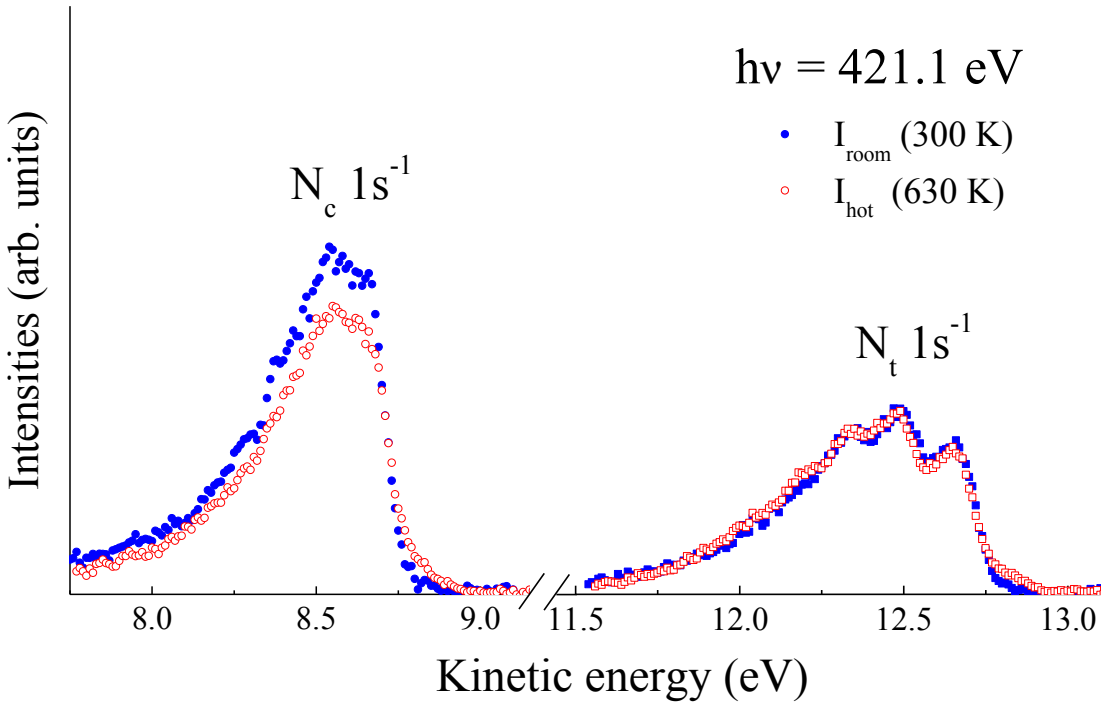

Figure 2. N_c and N_t K-shell photoelectron spectra of N_2O at a photon energy of 421.1 eV. Open (red) and Closed (blue) symbols represent intensities of photoelectrons at 630 K and at room temperature (300 K), respectively. See text for more information.

2.2 Decomposition procedure for the initial-vibrational-level-specific photoelectron spectrum

The core-level PESs measured at two different temperatures of 300 and 630 K as shown in figure 2, may be assumed to be comprised of two PESs corresponding to two different vibrational levels in the initial ground electronic state. In the case of the N_2O, the lowest vibrationally-excited level has an excitation energy of 73 meV [27, 28] above the vibrationally-ground level and corresponds to a bending excitation, v_2 = 1 i.e., (0 1 0). Thus, one PES is from the ensemble of molecules in the vibrationally-ground level of Σ-symmetry, which may be regarded as a linear molecule (0 0 0). The other is from molecules in the vibrationally-excited level of Π-symmetry, which may be regarded as a bent molecule (0 1 0). The populations of these ensembles are given by the Boltzmann distribution at the given temperatures, which correspond to 300 and 630 K in the present measurements. The population of the vibraitonally-ground level at 300 and 630 K in the Boltzmann distributions were estimated to be 88 % and 55 %, whereas those in the vibrationally (bending)-excited level v_2 = 1, to be 10 % and 29 %, respectively. The initial populations of N_2O molecules in each vibrational level at 300 and 630 K as well as their excitation energies and symmetries are presented in table I [27, 28]. In table I, the vibrational fundamental modes, v_1, v_2, and v_3 represent the quasi-symmetric stretching, bending and quasi-antisymmetric stretching vibrations, respectively.

Table I. The vibrational excitation energies of the N_2O molecule and their Boltzmann distribution probabilities at room temperature, P (300 K) and at high temperature, P (630 K) [27, 28]. Vibrational modes, v_1, v_2, and v_3 represent the quasi-symmetric stretching, bending and quasi-antisymmetric stretching vibrations, respectively.

(v_1, v_2^l, v_3)	Symmetry	Degeneracy	Energy (eV)	P (300 K)	P (630 K)
$(0, 0^0, 0)$	Π	1	0.000	0.884	0.549
$(0, 1^1, 0)$	Σ^+	2	0.073	0.105	0.286
$(0, 2^0, 0)$	Σ^+	1	0.145	0.003	0.038
$(0, 2^2, 0)$	Δ	2	0.147	0.006	0.073
$(1, 0^0, 0)$	Σ^+	1	0.159	0.002	0.029
$(1, 1^1, 0)$	Π	2	0.232	0.000	0.015
$(0, 0^0, 1)$	Σ^+	1	0.276	0.000	0.003
$(1, 2^0, 0)$	Σ^+	1	0.305	0.000	0.002

$(2, 0^0, 0)$	Σ^+	1	0.318	0.000	0.002
$(0, 1^1, 1)$	Π	2	0.347	0.000	0.002

Solving the two coupled-equations below using the populations of vibrational levels at each temperature shown in table I and the PES measured at 300 and 630 K, I_{room} and I_{hot}, photoelectron spectra from vibrationally-ground and -excited levels, I_{ground} and I_{excited} can be obtained as follows:

$$I_{\text{room}}(300\text{ K}) = \text{P}_{\text{g}}(300\text{ K}) \times I_{\text{ground}} + \text{P}_{\text{ex}}(300\text{ K}) \times I_{\text{excited}}$$

$$I_{\text{hot}}(630\text{ K}) = \text{P}_{\text{g}}(630\text{ K}) \times I_{\text{ground}} + \text{P}_{\text{ex}}(630\text{ K}) \times I_{\text{excited}}$$

where $\text{P}_{\text{g}}(T)$ and $\text{P}_{\text{ex}}(T)$ are the populations of vibrationally-ground and -excited levels at a given temperature, T, in the Boltzmann distribution, respectively (see table I). In the present analysis, we employed the expression $\text{P}_{\text{ex}}(630\text{ K}) = 1 - \text{P}_{\text{g}}(630\text{ K})$ and solved the coupled equation. Then I_{excited} corresponds to a photoelectron spectrum from the contributions of all vibrationally excited levels. The contributions from $v_2 = 0$ and $v_2 = 1$ to I_{excited} at 630 K are ~55% and ~29%, respectively. The remaining (~16 %) may be negligible in the context of the following discussion of the results. We make use of I_{ground} and I_{excited} to obtain the initial-vibrational-level-specific PESs.

We note that no photoelectron from N_2 or NO molecule produced by thermal dissociation at high temperature (630 K) has been observed in these spectra, because the kinetic energy of emitted electrons from N_2 or NO are different from that of parent N_2O [5, 9].

3 Results and Discussion

3.1 Theoretical computations

For this study we have performed additional calculations based on previously published results [12, 19]. Vibrationally specific core ionization cross sections were computed using the Chase adiabatic approximation [29]. Thus we have computed the fixed-nuclei dipole photoionization matrix elements on a grid of geometries of the molecule. The vibrationally specific cross sections were then obtained by an integral of the product of initial and final vibrational states with the geometry dependent dipole matrix elements.

To consider the relative importance of hot band photoionization from the target N_2O molecule when the quasi-symmetric stretching mode is excited, fixed-nuclei photoionization calculations involving only linear geometries were performed. We could thus use the more accurate multichannel Schwinger configuration interaction (MCSCI) method [30, 31]. In this approach the bound states, i.e. the initial N electron state, and the final N-1 electron ionized states are represented by configuration interaction (CI) wave functions. The scattering state is then represented using a close-coupling wave function constructed from a sum of products of ion states and one-electron channel continuum functions. The details of the calculations were the same as in our previous study of the stretching modes in vibrationally specific core ionization of N_2O [12].

The calculations involving excitation of the bending modes, and thus bent geometries in the

fixed-nuclei calculations, used a single-channel HF-like treatment of the scattering problem leading to what we will refer to as equivalent-core Hartree-Fock (ECHF) results [19]. At each geometry, the cross section was computed using the single-channel static-exchange correlation-polarization model [32-34] where the targets were represented by the effective core approximation [35, 36]. In these calculations, the specific parameters used were the same as in our previous study of the bending modes in the core ionization of N_2O [19].

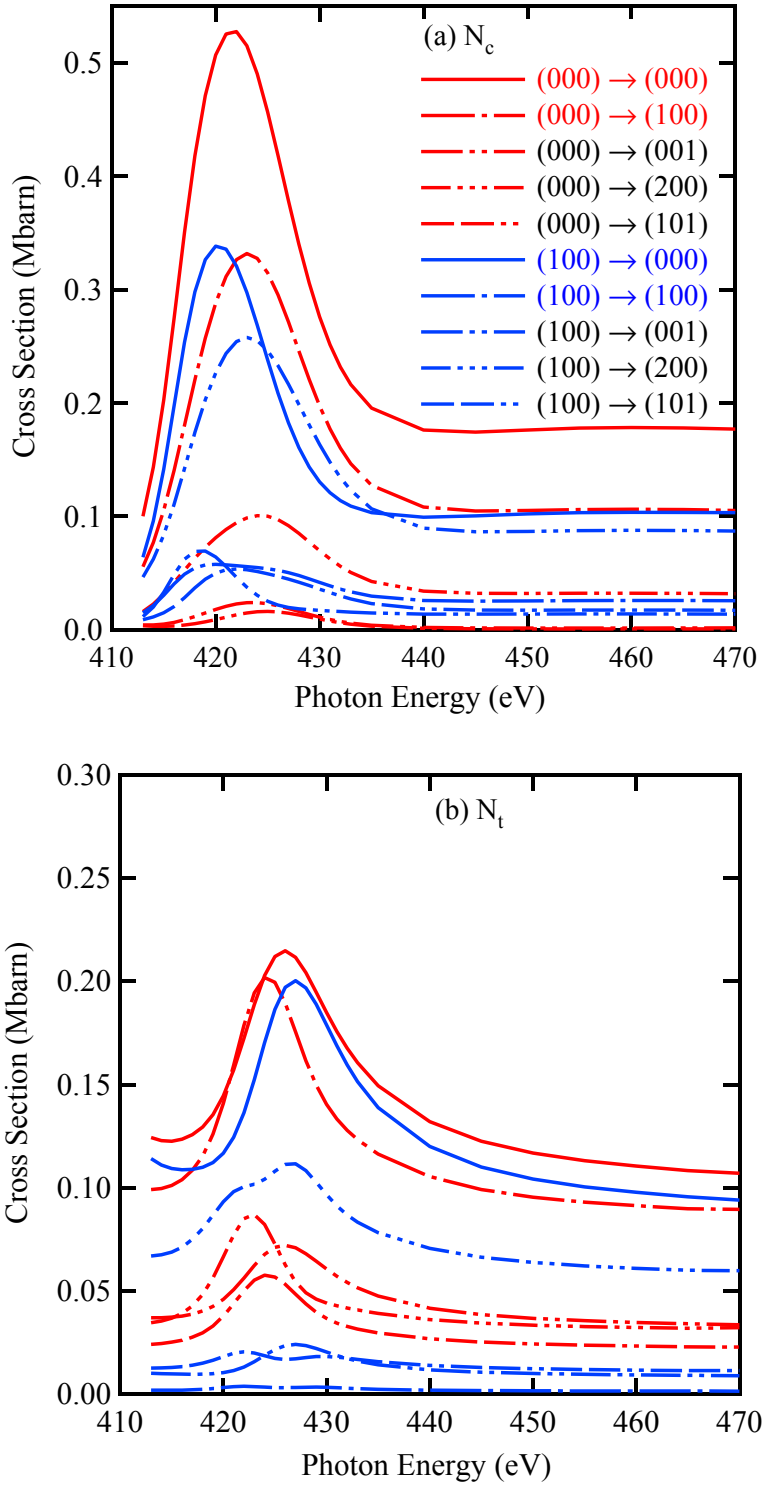

Figure 3. Computed site-specific cross sections for Nc and Nt K-shell ionization from the ground vibrational state (0 0 0) to various stretching states of the ion and the corresponding cross sections for ionization for the first stretching excited state (1 0 0) of the neutral target.

In figure 3, we show the vibrationally specific cross sections for ionization from the ground vibrational state (0 0 0) to various stretching states of the ion and the corresponding cross sections for ionization for the first stretching excited state (1 0 0) of the neutral target. The most notable feature of both the N_c and N_t results is that the intensity ratio (1 0 0)→(1 0 0)/(1 0 0)→(0 0 0) for ionization from the excited stretch state is much weaker than the corresponding ratio for ionization from the ground state, (0 0 0)→(1 0 0)/(0 0 0)→(0 0 0). Thus to fit the initial-vibrational-level-specific PES from the vibrationally-excited molecule, as performed below, it is important to include the (1 0 0) state population and to use appropriate Franck-Condon factors for the ionization from the (1 0 0) state which are different from the corresponding values for the ionization from the (0 0 0) state.

3.2 Initial-vibrational-level-specific PESs

Figures 4a and 4b depict the initial-vibrational-level-specific PESs, I_{ground} and I_{excited}, for N_c and N_t K-shell photoionization at a photon energy of 421.1 eV extracted from the spectra in figure 2 using the coupled-equations as mentioned above. The lowest lines in figures 4a and 4b, the difference (data-fit) spectrum for I_{excited}, provide a visual measure for evaluating the unfolding procedure. The structures of the difference spectra are due to a combination of noise in the data, a slight error of the energy axis of the digital nature of the data, deviations of the instrumental profile assumed in the analysis, and any breakdown in the Franck-Condon principle. At first glance, the profile of the I_{ground} and I_{excited} seem to be similar for N_c while they are significantly different for N_t. Below we will extract this difference employing the spectral line fitting procedure described elsewhere [4-10].

First, we focus on I_{ground}. Solid (blue) curves in figures 4a and 4b are a good fit to I_{ground} (full blue dots in figures 4a and 4b) and are the result of fitting employing the procedure described in the previous studies for N_2O molecules [12, 37]. Briefly, for both N_c and N_t, PESs of the vibrationally-ground level, I_{ground}, were fitted using the PCI-distorted line profiles convoluted with the Gaussian profile as described in details elsewhere [4-10]. I_{ground} can be fitted by a single progression of quasisymmetric vibrations (v_1' 0 0) for N_c and by combinations of quasi-symmetric and quasi-antisymmetric vibrations (v_1' 0 v_3') for N_t [12]. We fixed the vibrational frequencies, ω_{e1} = 136 meV for N_c and ω_{e1} = 178 meV and ω_{e3} = 303 meV for N_t. We also fixed a Lorentzian width 118 meV for both N_c and N_t [37]. The energy of the first peak (0 0 0) (i.e., vibrationally-ground level of ionic state, v_1'= v_2' = v_3' = 0), the intensity ratios of the individual vibrational components and the Gaussian width were regarded as fitting parameters because these values depend on the experimental conditions such as photon energy. The Gaussian width obtained from the present fitting was ~70 meV (FWHM) and consistent with the value estimated from a convolution of the monochromator bandwidth, the electron analyzer resolution and the Doppler broadening under the present experimental conditions. As

shown in figures4a and 4b (blue symbols and lines), the present PES from the vibrationally-ground level measured both for both N_c and N_t are well reproduced by the fits. The branching ratios to the individual vibrational levels of the core-hole state extracted from the fitting are in reasonable agreement with the values reported previously for room temperature N_2O [12], though the uncertainty of the ratios were significantly larger for the present data than the previous ones due to lower statistics.

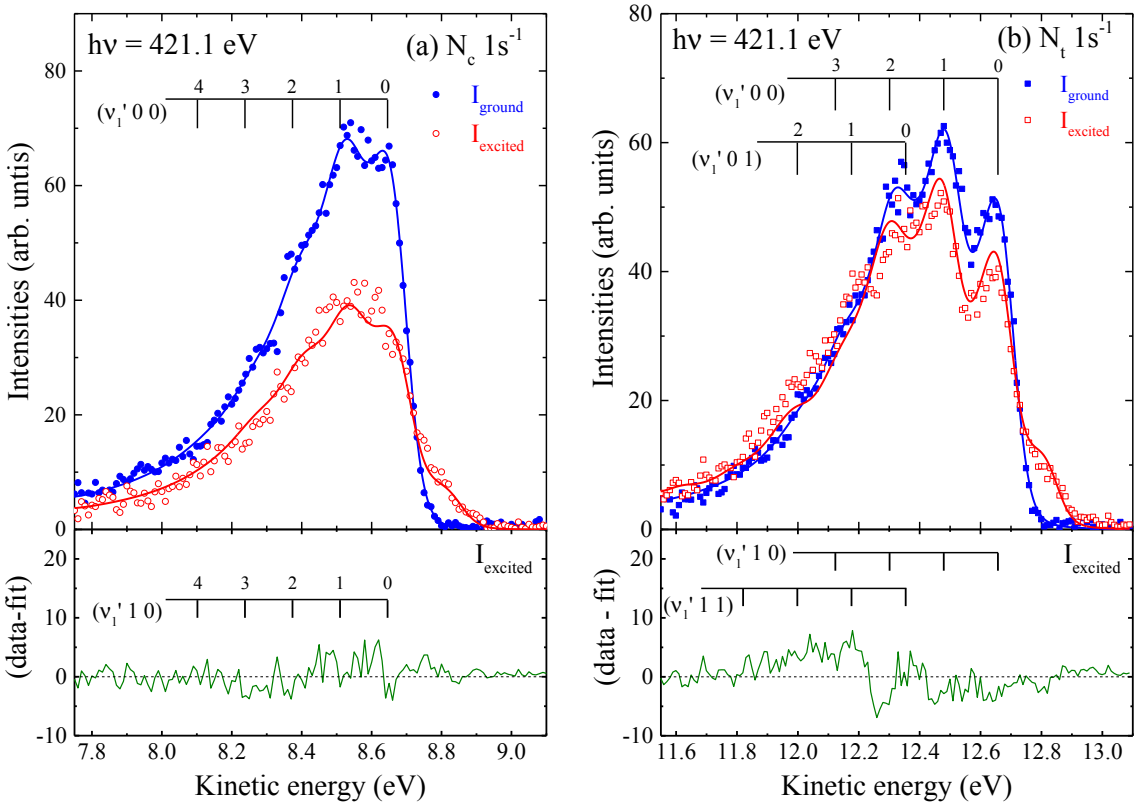

Figure 4. Initial-vibrational-level-specific photoelectron spectra, I_{ground} (blue) and I_{excited} (red), at a photon energy of 421.1 eV extracted from the spectra in figure 2. The solid curves in the upper panels show the fitting results based on the parameters obtained from the previous measurements [12, 37] (see text). The assignment combs indicate the positions of the transition starting from the (0 0 0) state. The bottom panels show the intensity difference between the present experimental PES and their fitting curve (data – fit) in the I_{excited} (red). The difference plots have the same vertical scale as the intensities given in the corresponding intensity plots in upper panels. The assignment combs in the lower panels show the position of the transitions starting from the (0 1 0) state.

Next, we focus on I_{ecxited} of N_c in figure 4a. A hot-band transition is clearly observed at ~8.8 eV, which is ~147 meV above the (0 0 0) main peak of I_{ground}, whereas the overall intensity profile is similar to I_{ground} of N_c. This energy interval corresponds approximately to either twice the excitation energy of the first bending level ($2v_2$ ~ 146 meV) or close to the first quasi-stretching level (v_1 ~ 159 meV) from the vibrationally-ground level of N_2O. This result indicates that the $(0\ 2\ 0) \rightarrow (0\ 0\ 0)$ and/or $(1\ 0\ 0) \rightarrow (0\ 0\ 0)$ deexcitations are induced. In the present calculation, however, we found that

the bending quantum number changing transitions, $(0\ 2^0 0) \rightarrow (0\ 0\ 0)$ are about 100 times weaker than the related photoionization transitions where the bending quantum numbers do no change. Therefore, I_{excited} of N_c may include two vibrational progressions, one from the ionization of the first bending excited level (0 1 0) to a progression of (v_1' 1 0) for the N_c core-hole state and the other from the ionization of the quasi-symmetry stretching excited level (1 0 0) to (v_1' 0 0). The vibrational-excited levels in the initial electronic ground state may affect the shape resonance as discussed in Ref. [19]. Then, in general, the intensity distributions for the two progressions $(0\ 1\ 0) \rightarrow (v_1'\ 1\ 0)$ and $(1\ 0\ 0) \rightarrow (v_1'\ 0\ 0)$ in I_{ecxited} may differ from those from $(0\ 0\ 0) \rightarrow (v_1'\ 0\ 0)$ in I_{ground}. However, the two vibrational progressions are overlapped almost completely except for $(1\ 0\ 0) \rightarrow (0\ 0\ 0)$, since the energy difference (~147 meV) between the $(0\ 1\ 0) \rightarrow (v_1'\ 1\ 0)$ and $(1\ 0\ 0) \rightarrow (v_1'\ 0\ 0)$ is close to the quasi-symmetric vibrational energy (~159 meV). As a result, we could not perform a reasonable fitting to I_{excited} treating relative intensities of the vibrational components as independent fitting parameters. Instead, we performed the fitting to I_{excited} of N_c using the relative intensity ratios of $(0\ 0\ 0) \rightarrow (v_1'\ 0\ 0)$ obtained for I_{ground} for the vibrational progressions $(0\ 1\ 0) \rightarrow (v_1'\ 1\ 0)$ and the Franck-Condon factors calculated in the present computation for the $(1\ 0\ 0) \rightarrow (v_1'\ 0\ 0)$ as described in Section 3.1. Vibrational frequencies and also the line widths were also assumed to be the same for I_{excited} and I_{ground}. In addition, we fixed the position of the peak (0 1 0) in I_{excited} to be the same as that of (0 0 0) in I_{ground}. The fitting result is shown in figure 4a (red line) where we see a reasonable fit to I_{excited}. The deviation of the experimental data from the fit was also included in the bottom panel of figure 4a. This deviation can be regarded as a measure of changes in the final state vibrational distributions due to quasi-symmetry stretching excitation in the initial state. We conclude that the present deconvolution procedure using the Franck-Condon factors calculated for $(1\ 0\ 0) \rightarrow (v_1'\ 0\ 0)$ gives a reasonable fit for the N_c core level, because no deviation was observed within the experimental statistical uncertainties in figure 4a.

Finally, we focus on I_{excited} of N_t in figure 4b. The peak at the highest kinetic energy ~12.8 eV is assigned, as described above for N_c to the hot-band transition $(1\ 0\ 0) \rightarrow (0\ 0\ 0)$. Comparison of the fitted curve with the experimental points, and examination of the difference plot, leads to the conclusion that the same approach as one carried out for N_c generally does very well also in the fitting spectrum for N_t over the entire kinetic energy range. In more detail, as also depicted in figure 4b, a weak systematic-structure remained in the difference plot, contrary to the variation in figure 4a, corresponds to the kinetic energy positions of $(v_1'\ 1\ 0)$ and $(v_1'\ 1\ 1)$ transitions, which is still an open question in the present analysis.

3.3 Partial cross section of nitrogen K-shell ionization

Integrating the initial-vibrational-level-specific PES in figures 4a and 4b over all different vibrational components at each photon energy, we can obtain the relative partial cross sections of the vibrationally-ground and bending-excited levels for N_c and N_t K-shell photoionization as a function of photon energy. Figures 5a and 5b show the initial-vibrational-level-specific partial cross sections

σ_{ground} and σ_{bend} from vibrationally-ground and bending-excited levels, respectively, together with the previous experimental results measured at room temperature [11, 12] and the present theoretical calculations. The present relative cross section, σ_{ground} for N_c K-shell ionization was normalized to the absolute scale of that measured by Lucchese et al. [12] at the resonant peak around ~423 eV. Other relative cross sections, σ_{ground} for N_t K-shell ionization and σ_{bend} for both ionization, were scaled to the σ_{ground} for the N_c K-shell ionization. The cross sections for N_c and N_t K-shell ionizations measured at room temperature are assumed to be the present cross sections from the vibrational ground state, because ~88 % of the molecules are in the ground vibrational state in the Boltzmann distribution (see table I). Note that the present 6 data points are connected by approximate polynomial curves as shown in figures 4a and 4b.

3.3.1 Partial cross sections from vibrationally-ground level

For both N_c and N_t K-shell photoionization as shown in figures 5a and 5b, the partial cross sections from the vibrationally-ground level (0 0 0) are in reasonable good agreement with the previous experimental results, i.e., vibrationally-integrated cross sections measured at room temperature [12], whereas a small deviation is seen below 426 eV from the data of Schmidbauer et al [11]. More precisely, our previous measurement at room temperature was performed at high resolution, ~ 50 meV, to obtain the vibrationally-resolved partial cross sections for the final vibrational levels of core-hole states whereas the total energy resolution claimed in the cylindrical mirror analyzer used by Schmidbauer et al. [11] was ~2 eV. As shown in figures 5a and 5b, differences between two previous cross sections around ~420 eV might be ascribed partly to this energy resolution together with the transmission efficiency of the spectrometers.

A broad enhancement is clearly shown around ~426 eV in both cross sections for N_c and N_t K-shell ionizations, characterizing the typical σ shape resonance which has been previously discussed [11, 12]. In Ref. 12, we demonstrated that the shape resonance energies are sensitive to the final ionic vibrational level in the vibrationally-resolved partial cross sections. The reason is that the shape resonance is sensitive to the internuclear distances between the neighboring atoms. Note that the resonant enhancement for N_t is less prominent than that for N_c. A shallow shoulder around ~418 eV in figures 5a and 5b may correspond to the doubly-excited state assigned previously as N_c $1s^{-1}1\pi^{-1}$ to $(\pi^*)^2$ from angle-resolved ion yield spectroscopy [38]. This feature was also observed experimentally in K-shell photoelectron spectra for the vibrationally-resolved partial cross sections for the final vibrational levels by Lucchese et al [12], and in the initial vibrational-level specific, symmetry-resolved ion-yield spectra of Tanaka et al [19], although it has not yet been fully discussed. Similar structures attributed to the doubly-excited state were observed in the partial cross sections of nitrogen K-shell photoionization for N_2 molecules [5]. In addition to the σ resonance around a photon energy of ~426 eV, there is a lower-energy σ resonance predicted theoretically near threshold in some cross sections for N_t [19], indicated by the fact that the computed fixed-nuclei cross section becomes larger as the bending angle increases (figure 3 in Ref. 19). Although our present experimental data do not extend down to

threshold, the observed cross section is seen to decrease towards the threshold.

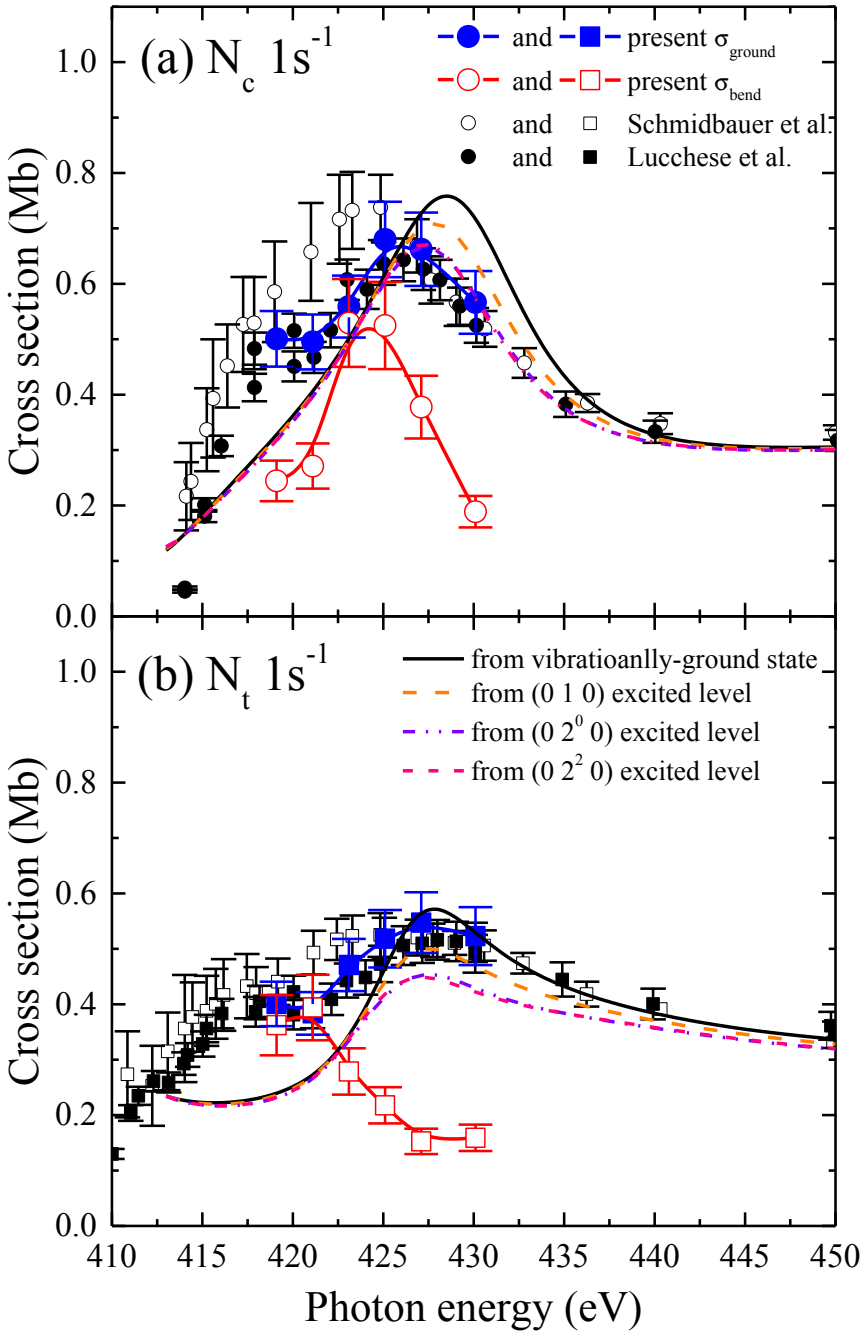

Figure 5. The initial-vibrational-level-specific cross sections of N_c and N_t K-shell ionizations from bending-excited (v_2" = 1) and vibrationally-ground (v_2" = 0) levels. Solid (blue) and open (red) symbols: present experimental results from the vibrationally-ground level and bending-excited level, respectively. Solid (black) symbol: Lucchese et al. [12] at room temperature. Open (black) symbol: Schmidbauer et al.[11] at room temperature. Solid curve (black), dashed curve (orange), dashed-dotted (purple) and double-chained (pink) curves: Ionization cross sections summed over the final vibrational

levels from the vibrationally-ground (0 0 0) level and (0 1 0), (0 2^0 0), and (0 2^2 0) bending-excited levels.

3.3.2 Partial cross sections from bending-excited level

In the N_c K-shell photoionization as shown in figure 5a (red symbols and curves), the partial cross section from the bending-excited levels, σ_{bend}, shows again a resonant enhancement at a photon energy of ~424 eV but the peak position is shifted about ~2 eV to the lower photon energy side with a decrease in width (from ~4.9 eV to ~4.0 eV) compared to the ground level, σ_{ground}. These results suggest that the energy position and the width of the shape resonance in N_c K-shell ionization of N_2O are sensitive to not only the bond length [3-10] in final core-ionized states but also to the bending angle in initial states. This feature is consistent with the present additional calculations based on the results previously reported [12, 19]. Such a shift in the peak of a resonant feature has been observed previously in the σ shape resonance regions above ionization thresholds in the angle-resolved ion yield [19]. It may be worth noting that similar energy shifts were observed also for the resonant energies of the π-resonances for the $C1s^{-1}2\pi_u$, $O1s^{-1}2\pi_u$ and N $1s^{-1}3\pi$ [16, 17] of hot-CO_2 and hot-N_2O molecules. It is of interest to the present discussion that in low energy electron scattering, we have also observed similar shifts in resonant parameters for vibrational excitations from initial vibrationally-ground and bending-excited levels of hot-CO_2, -N_2O, and -OCS [13-15].

In figure 5b, the cross section from the bending-excited levels for N_t increases monotonically in a "bell shape" from 430 eV towards ~ 419 eV as the photon energy decreases, indicating presumably that the σ resonance enhancement has been shifted by ~6 eV to the lower energy side from the vibrationally-ground level at ~426 eV. The tendency of the cross section from the bending-excited (0 1 0) state is surprisingly different from that of the vibrationally ground (0 0 0) state for N_t and also from that of the bending excited state for N_c. Here, we are convinced that such a large difference observed in only the σ_{bend} for the N_t ionization is very unlikely to be caused by the present experimental error because of our simultaneous measurement of both N_c and N_t photoelectrons as shown in figure 2. Another reason for our confidence is that, as in figure 5b, the present partial cross section from the vibrationally-ground level for N_t reproduced nicely the experimental results [12] measured at room temperature within the experimental uncertainty. Therefore, though we could not identify decisively the shape resonance energy since the photon energy range of present measurement has a lower limit of 419 eV, we may conclude with confidence that the downshift of the shape resonance for N_t is much more pronounced than for N_c. The enhancement of the downshift for N_t in comparison with that for N_c qualitatively agrees with the theoretical prediction in the present calculations, though the experimentally observed downshift is larger than the prediction.

As described above, for both shape resonances associated with the N_c and N_t core-holes, we experimentally found that the resonant energies are shifted to lower energy and the resonant widths become narrower for the bending-excited levels compared to those for the vibrationally-ground level. The difference in the sensitivity of the shape resonance to bending when comparing the N_t and N_c hole

states may be explained by considering the effective core (EC) picture for the ion states formed in this process [19]. In the case of $(1s)^{-1}$ N_t, hole state, the valence orbitals are represented by those of the $(ONO)^+$ molecule, whereas for the $(1s)^{-1}$ N_c hole state, the valence state is approximated by that of the $(NOO)^+$ molecule. Thus in the case of the N_t, hole, bending leads to a significant change in the electron-molecule interaction potential since in the linear geometry the state has approximately a $D_{\infty h}$ symmetry which has no dipole moment whereas in the bent geometry there is a dipole in the perpendicular direction. In the case of the N_c hole state, the linear geometry already has a dipole moment so that bending does not involve such a significant change in the electron-molecule interaction potential. This difference between the N_c and N_t may explain the more significant changes observed in the cross sections when the molecule bends for the N_t hole compared to the N_c hole. More detail on the reasons for the shift down of the shape resonance energy and the narrowing of the profiles may be found in Ref. 19.

3.4 Asymmetry parameter of nitrogen K-shell ionization

Based on the coupled-equations described in Sec 2.2, angle-resolved PES of vibrationally-excited (0 1 0) and vibrationally-ground (0 0 0) levels were obtained from the PES recorded at 300 and 630 K, and for two directions 0^o and 90^o with respect to the linear polarization vector of the incident photons. Integrating those angle-resolved PES at each photon energy, we can obtain the asymmetry parameter from the vibrationally-ground and bending-excited levels for N_c and N_t K-shell photoionization as a function of photon energy. Figures 6a and 6b show the asymmetry parameter, β parameter for N_c and N_t K-shell photoionization obtained from the initial-vibrational-level-specific PES recorded at 0^o and 90^o with respect to the polarization vector of incident photon. Not only the β parameter obtained from vibrationally-ground I_{ground} but also that from bending-excited $I_{excited}$ agree with both the previous measurements at room temperature [11, 12]. We found that the present calculated β parameter (black, orange, blue, and pink lines) based on the equivalent-core Hartree Fock method can reproduce the photon energy dependence on the experimental initial-vibrational-specific results for N_c and N_t K-shell ionizations. The energy dependence of the partial cross sections between σ_{ground} and $\sigma_{excited}$ are different for N_c and N_t K-shell ionizations, whereas the emission directions of inner-shell electrons do not change due to the initial bending-excitation in N_2O. The present additional computed β parameter qualitatively reproduced the experimental trend for both N_c and N_t core-hole levels.

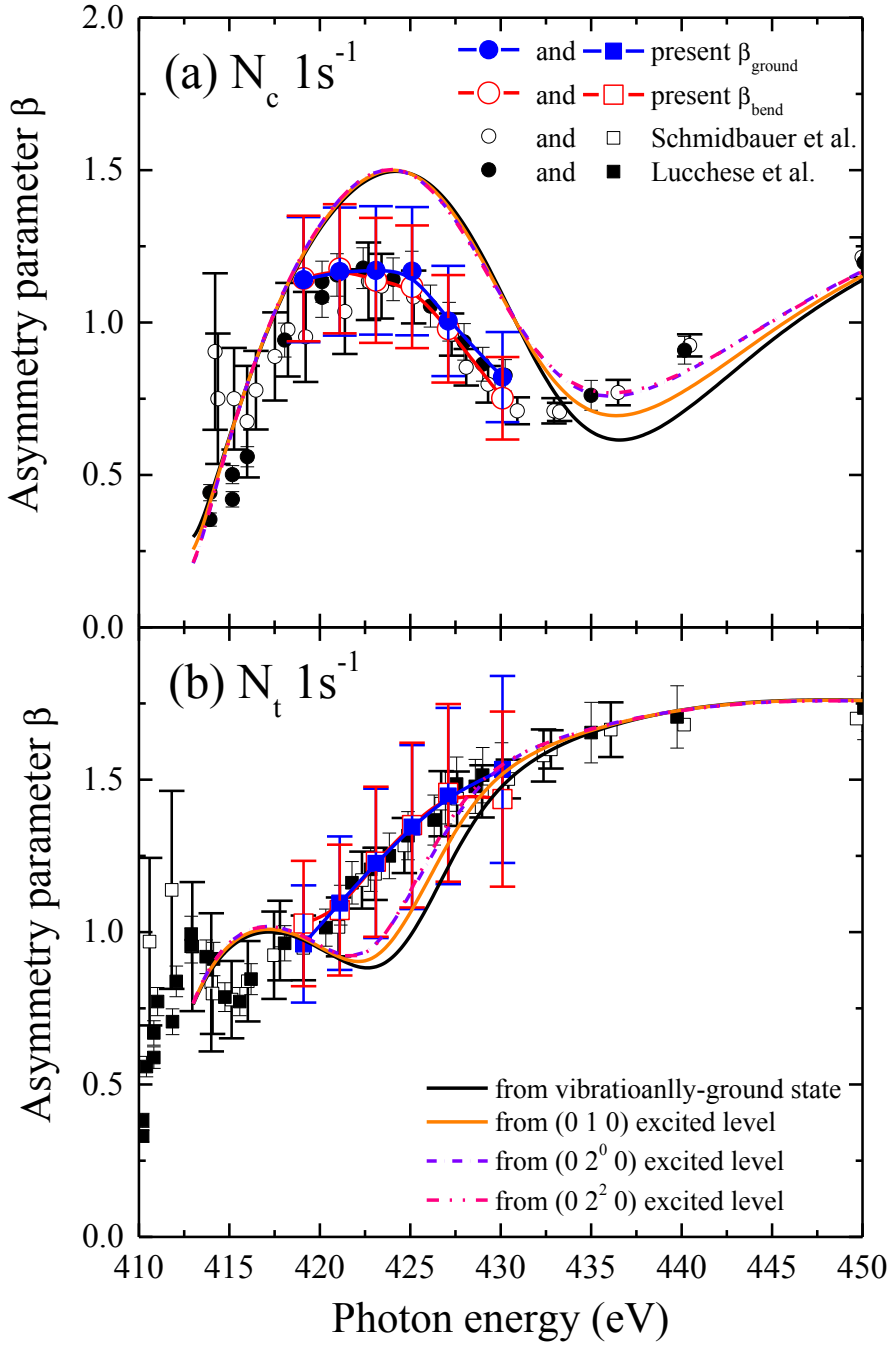

Figure 6. Asymmetry parameter, β for N_c and N_t K-shell photoionization obtained from the initial-vibrational-level-specific PESs recorded at 0^o and 90^o with respect to the polarization vector of incident photon. Solid (blue) and open (red) symbols: present experimental results from vibrationally-ground level and bending-excited level, respectively. Solid and open (black) symbols: experimental results of Lucchese et al. [12] and Schmidbauer et al. [11] at room temperature. Solid curve (black), dashed curve (orange), dashed-dotted (purple) and double-chained (pink) curves: Asymmetry parameters summed over the final vibrational levels from the vibrationally-ground (0,0,0) state and (0,1,0), $(0,2^0,0)$, and $(0,2^2,0)$ bending-excited levels.

4 Conclusion

Photoelectron spectra for the center (N_c) and terminal (N_t) nitrogen K-shell photoionization of N_2O molecule in the photon energy region of 419 eV – 430 eV have been measured at room temperature (~300 K) and a high temperature (~630 K). Using vibrational populations based on the Boltzmann distribution at these temperatures, photoelectron spectra for specific initial ground and bending-excited levels (initial-vibrational-level-specified PES) were extracted in the σ shape resonance region. Partial ionization cross sections and asymmetry parameters from vibrationally-ground and bending-excited levels for N_c and N_t K-shell photoionizations were also obtained as a function of incident photon energy by integrating the initial-vibrational-level-specified PES over all vibrational levels in the final state at each photon energy and were compared with additional calculations based on previously published results [12, 19]. For N_c K-shell photoionization, the energy position and the width of the shape resonance from bending-excited levels was found to be shifted to the lower photon energy side and became narrower than those from the vibrationally-ground level. Furthermore, in the partial cross section from bending-excited levels for N_t core-ionization, the shape resonance energy is drastically shifted to the much lower energy side compared with that for N_c photoionization. The bending angles as well as the symmetry breaking in the initial vibrational level was found to strongly affect the shape resonance in N_t photoionization. All these findings are consistent with the present additional calculations based on results reported in our previous paper [19], though the energy shifts of the shape resonance observed experimentally here are larger than the computed theoretical shifts and the observed experimental shifts seen in the ARIY spectra [19]. On the other hand, the present experimental data show that the asymmetry parameters of N_c and N_t K-shell ionizations are independent of the initial vibrational states in the shape resonance region. Finally, although the present study clearly identified the impact of bending vibrations in the initial state on site-specific shape resonances, vibrationally-resolved photoelectron spectroscopy of vibrationally-excited (bending) molecules at higher resolution with better statistics, as well as further theoretical studies will be desired to fully understand further details of the problems discussed here.

5 Acknowledgments

This experiment was carried out with the approval of the SPring-8 program review committee (Proposal's No. 2011A1094 and 2011B1576). All of authors thank Dr. Yusuke Tamenori and Dr. Itaru Higuchi for their technical support during our beamtime at BL27SU in these projects. This study was supported by Grants-in-Aid for Scientific Research from the Japanese Society for Promotion of Science (Grants No. 23540468). The work at Texas A&M University was supported by the United States Department of Energy, Office of Science, Basic Energy Science, Geoscience, and Biological Divisions, under Award No. DE-SC0012198 and by the Robert A. Welch Foundation (Houston, Texas) under Grant No. A-1020. Also, the assistance and computer time provided by the Supercomputing Facility at Texas A&M University are acknowledged.

References

[1] Dehmer J L, Dill D and Parr A C 1985 *Photophysics and Photochemistry in the Vacuum Ultraviolet edited by McGlynn S, Findly G, Huebner R (Reidel, Dordrecht)* 341

[2] Dehmer J L, Dill D and Wallace S 1979 *Phys. Rev. Lett.* **43** 1005

[3] Hargenhahn U 2004 *J. Phys. B: At. Mol. Opt. Phys*. *37* R89 and references therein

[4] De Fanis A, Mistrov D A, Kitajima M, Hoshino M, Shindo H, Tanaka T, Tanaka H, Tamenori Y, Pavlychev A A and Ueda K 2005 *Phys. Rev.* A **71** 052510

[5] Semenov S K, Cherepkov N A, Matsumoto M, Fujiwara K, Ueda K, Kukk E, Tahara F, Sunami T, Yoshida H, Tanaka T, Nakagawa K, Kitajima M, Tanaka H and De Fanis A 2006 *J. Phys. B: At. Mol. Opt. Phys.* **39** 375

[6] Hoshino M, Nakagawa K, Makochekanwa C, Tanaka T, Kuze N, Matsumoto M, Fujiwara K, De Fanis A, Tamenori Y, Kitajima M, Tanaka H and Ueda K 2006 *Chem. Phys. Lett*. **421** 256

[7] Hoshino M, Nakagawa K, Tanaka T, Kitajima M, Tanaka H, De Fanis A, Wang K, Zimmermann B, McKoy V and Ueda K 2006 *J. Phys. B: At. Mol. Opt. Phys.* **39** 3047

[8] Hoshino M, Nakagawa K, Tanaka T, Kitajima M, Tanaka H, De Fanis A, Mistrov D A, Brykalova X O, Pavlychev A A, Hatamoto T and Ueda K 2006 *J. Phys. B: At. Mol. Opt. Phys*. **39** 3655

[9] Hoshino M, Montuoro R, Lucchese R R, De Fanis A, Hergenhahn U, Prümper G, Tanaka T, Tanaka H and Ueda K 2008 *J. Phys. B: At. Mol. Opt. Phys.* **41** 085105

[10] Hopper D G 1984 *J. Chem. Phys*. **80** 4290

[11] Schmidbauer M, Kilcoyne A L D, Randall K J, Feldhaus J, Bradshaw A M, Braunstein M and McKoy V 1991 *J. Chem. Phys*. **94** 5299

[12] Lucchese R R, Söderström J, Tanaka T, Hoshino M, Kitajima M, Tanaka H, De Fanis A, Rubensson J E and Ueda K 2007 *Phys. Rev.* A **76** 012506

[13] Kato H, Kawahara H, Hoshino M, Tanaka H, Campbell L and Brunger M J 2008 *Chem. Phys. Lett.* **465** 31

[14] Kato H, Ohkawa M, Tanaka H, Shimamura I and Brunger M J 2011 *J. Phys. B: At. Mol. Opt. Phys.* **44** 195308

[15] Hoshino M, Ishijima Y, Kato H, Mogi D, Takahashi Y, Fukae K, Limão-Vieira P, Tanaka H and Shimamura I 2016 *Eur. Phys. J.* D **70** 100.

[16] Tanaka T, Makochekanwa C, Tanaka H, Kitajima M, Hoshino M, Tamenori Y, Kukk E, Liu X J, Prümper G and Ueda K 2005 *Phys. Rev. Lett.* **95** 203002

[17] Tanaka T, Hoshino M, Makochekanwa C, Kitajima M, Prümper G, Liu X J, Lischke T, Nakagawa K, Kato H, Tamenori Y, Tanaka H and Ueda K 2006 *Chem. Phys. Lett.* **428** 34

[18] Tanaka T, Hoshino M, Kato H, Harries J R, Tamenori Y, Ueda K and Tanaka H 2008 *J. Electr. Spectrosc. Relat. Phenom.* **164** 24

[19] Tanaka T, Hoshino M, Lucchese R R, Tamenori Y, Kato H, Tanaka H and Ueda K 2010 *New. J. Phys*. **12** 123017

[20] Ohashi H, Ishiguro E, Tamenori Y, Kishimoto H, Tanaka M, Irie M, Tanaka T and Ishikawa T 2001 *Nucl. Instrum. Methods Phys. Res.* A **467-468** 529

[21] Ohashi H, Ishiguro E, Tamenori Y, Okumura H, Hiraya A, Yoshida H, Senba Y, Okada K, Saito N, Suzuki I H, Ueda K, Ibuki T, Nagaoka S, Koyano I and Ishikawa T 2001 *Nucl. Instrum. Methods Phys. Res.* A **467-468** 533

[22] Ueda K 2003 *J. Phys. B: At. Mol. Opt. Phys.* **36** R1

[23] Tanaka T and Kitamura H 1996 *J. Synchrotron Radiat.* **3** 47

[24] Yoshida H, Senba Y, Morita M, Goya Y, De Fanis A, Saito N, Ueda K, Tamenori Y and Ohashi H 2004 *AIP Conf. Proc.* **705** 267

[25] Prince K C, Avaldi L, Coreno M, Camilloni R and de Simone M 1999 *J. Phys. B: A. Mol. Opt. Phys.* **32** 2551

[26] Alagia M, Pichter R, Stranges S, Agåker M, Ström M, Söderström J, Såthe C, Frifel R, Sorensen S, De Fanis A, Ueda K, Fink R and Rubensson J E 2005 *Phys. Rev.* A **71** 012506

[27] Shimanouchi T 1972 *Nat. Stand. Ref. Data Ser., Nat. Bur. Stand. (U.S.)* **39** 10

[28] Herzberg G 1945 *Molecular Spectra and Molecular Structure II. Infrared and Raman Spectra of Polyatomic Molecules* (Van Nostrand Reinhold Compnay, New York) 278

[29] Chase D M 1956 *Phys. Rev.* **104** 838

[30] Stratmann R E, Zurales R W and Lucchese R R 1996 *J. Chem. Phys.* **104** 8989

[31] Stratmann R E and Lucchese R R 1995 *J. Chem. Phys.* **102** 8493

[32] Perdew J P and Zunger A 1981 *Phys. Rev. B* **23** 5048

[33] Natalense A P P and Lucchese R R 1999 *J. Chem. Phys.* **111** 5344

[34] Gianturco F A, Lucchese R R and Sanna N 1994 *J. Chem. Phys.* **100** 6464

[35] Thomas T D, Saethre L J, Sorensen S L and Svensson S 1998 *J. Chem. Phys.* **109** 1041

[36] Dobrodey N V, Köppel H and Cederbaum L S 1999 *Phys. Rev. A* **60** 1988

[37] Ehara M, Tamaki Y, Nakatsuji H, Lucchese R R, Söderström J, Tanaka T, Hoshino M, Kitajima M, Tanaka H, De Fanis A and Ueda K 2007 *Chem. Phys. Lett.* **438** 14

[38] Adachi J, Kosugi N, Shigemasa E and Yagishita A 1995 *J. Chem. Phys*. **102** 7369